CMS Draft Analysis Note

2010/11/30
Head Id: 1.0
Archive Id:
Archive Date:

Search for Collimated Groups of Muons

Jim Pivarski, Alexei Safonov, Aysen Tatarinov

Abstract

We present an inclusive, signature-based search for groups of collimated muons, arising from spectroscopic cascades in a hidden sector accessible only through high-energy collisions, using the CMS detector. In several signatures defined by number of muons per collimated group and number of groups per event, we searched for the lightest state in the hidden spectrum with a mass-peak fit and set limits on $\sigma\mathcal{B}\alpha$, where α is the model acceptance of the signature. Depending on the signature and the mass of the lightest state ($2m_\mu$–5 GeV/c^2), new resonances are ruled out at the level of XX-YY pb for 95% C.L. We also set $\sigma\mathcal{B}$ limits on two representative benchmark models: SUSY dark matter with a $\mathcal{U}(1)_{\text{dark}}$ and NMSSM Higgs escaping LEP limits via Higgs-to-Higgs decays.

1 Introduction

1.1 Motivation

FIXME: Needs a lot of references.

Although the dimuon mass spectrum is well understood in e^+e^- and $p\bar{p}$ collisions up to 0.2 and 2 TeV respectively, (**FIXME:** get real numbers) new states may be hidden by weak couplings to Standard Model particles. A wide class of hidden-valley models predicts new states coupling weakly to the Standard Model yet significantly to a hidden sector, with strong mixing between the Standard Model and the hidden sector only for massive particles. In these scenarios, high collision energies are necessary to create massive particles M, but these particles can then decay through the whole spectrum to the lightest hidden state: $pp \to M\overline{M}$ and $M \to mX$ where m is the lightest hidden particle. If m is unstable, it would decay with very small width to the kinematically-accessible Standard Model states, either democratically (Z-like) or to the heaviest accessible state (Higgs-like). Muon-pair final states would appear as a low-mass, high-momentum dimuon resonance, and therefore be collimated by relativistic boost. With several low-mass states in the decay chain, e.g. $m_2 \to m_1 m_1 \to 4\mu$, cascades would either produce two groups of collimated dimuons or one group of four collimated muons, depending on the boost of m_2. Arbitrarily complex decay chains are conceivable, and groups of muons might be produced in association with other Standard Model pairs, such as e^+e^- and $\pi\pi$. These striking signatures are often called "lepton jets."

Hidden, low-mass resonances are especially interesting in light of the high-energy positron excess reported by the PAMELA primary cosmic-ray experiment. This excess of interstellar positrons could be the product of WIMP annihilations, assuming that the WIMP annihilation rate is higher than what would be expected from thermal freeze-out in the early universe, and also assuming some mechanism to prohibit decay chains that produce antiprotons, in which no excess was observed. A new force boson, z_{dark}, with a mass of approximately 1 GeV/c^2 and coupling significantly to WIMPs yet weakly to Standard Model particles, would explain both observations. Acting as a long-range Yukawa force, z_{dark} would draw together slow-moving WIMPs, increasing their effective annihilation cross-section in the modern era without affecting their production in the early universe. As a decay channel, $z_{\text{dark}} \to p\bar{p}X$ would be kinematically forbidden if the mass of z_{dark} were above 2 GeV/c^2 or so. Relatively simple extensions of this picture, such as adding a dark Higgs boson h_{dark} to give the z_{dark} its mass, or introducing the force with non-abelian structure, would produce more complex event topologies: 2^N fermion pairs per lepton jet for an N-state decay chain and/or several lepton jets per event.

Another, very different, motivation derives from the tension between the low Higgs mass predicted by precision electroweak fits and the direct LEP limit of 114 GeV/c^2. This limit assumes that the Higgs boson decays directly into Standard Model particles

with known branching fractions. If additional light Higgs bosons allow for Higgs-to-Higgs decays, the direct limit may be circumvented. In a well-defined region of Next-to Minimal SuperSymmetric (NMSSM) parameter space, the lightest CP-odd Higgs (a_1) can have arbitrarily low mass. Below the $2m_\tau$ threshold, the branching fraction for $a_1 \to \mu\mu$ is about 20%, making its detection in the muon channel visible. For values of the NMSSM parameters that give the lightest CP-even Higgs (h_1) a large singlet field component, $h_1 \to a_1 a_1$ can be as large as 100%. If nature has chosen this model, then the Higgs mass could be as low as 86 GeV/c^2 and the primary Higgs signature would be $h_1 \to a_1 a_1 \to 2\mu, 2\mu$, where the dimuons appear as well-collimated lepton jets.

1.2 Method

In this paper, we present an inclusive, signature-based search for collimated dimuons with $2m_\mu <$ mass < 5 GeV/c^2 arising from hidden cascade chains. Additional objects, such as isolated single leptons, hadronic jets, and missing energy, are neither included in the search nor are they forbidden. In particular, boosted dimuons are not rejected if they are overlapped by e^+e^- or $\pi\pi$ from other resonance decays in the same lepton jet, nor are they rejected due to activity from a nearby hadronic jet that might arise, for example, from SUSY cascade decays.

We assume that all decay chains in the hidden sector end with a low-mass state m_1 before decaying to opposite-sign muon pairs, though there may be several instances of this particle per event, possibly overlapping one another. This assumption is equivalent to assuming that the coupling between the hidden states and the Standard Model is much weaker than the couplings of the hidden states with each other. We therefore search for one new resonance with a single dimuon mass peak, after identifying the combination of muon pairs that is most likely to have arisen from distinct resonance decays.

Identifying the distinct dimuon resonances proceeds in two steps. First, nearby muons are grouped into "mu-jets" with an arbitrary number of muons per group. The definition of "nearby muons" is kinematic rather than geometric: two muons are considered near each other if their pairwise invariant mass is less than 5 GeV/c^2 with both muons satisfying a minimim-p_T threshold. This differs from selections based on a maximum $\Delta R = \sqrt{(\Delta\phi)^2 + (\Delta\eta)^2}$ because ΔR approximately corresponds to relativistic boost, effectively a tighter requirement on resonance momentum for higher resonance masses (see Fig. 1).

The second step in identifying distinct dimuon resonances is to split high-multiplicity mu-jets into a combination of pairs with nearly equal mass for all pairs. For example, a mu-jet containing four muons from $m_2 \to m_1 m_1 \to 4\mu$ has two potential combinations, and the combination with more nearly equal masses is much more likely to correspond to the true mass of m_1. We call the opposite-sign muon pairs after this step "fundamental dimuons," and there is only one candidate combination per event.

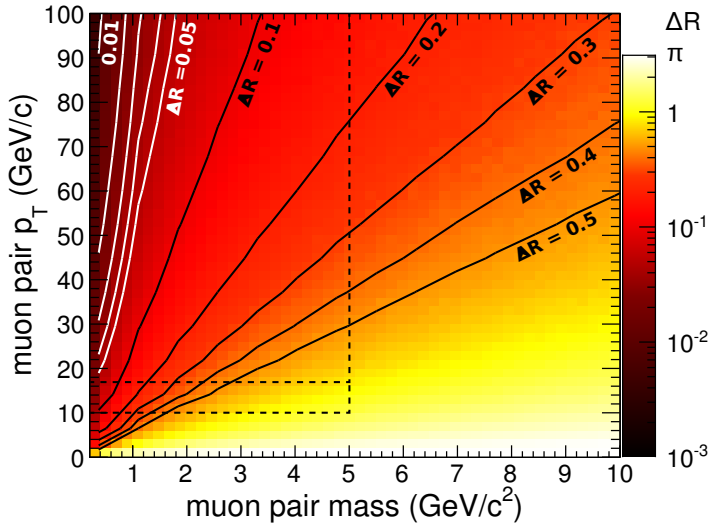

Figure 1: Relationship between ΔR (represented by color scale and contour lines) and the mass and momentum of a pair of muons (simple model: isotropic resonances decaying as scalars). Lines of constant relativistic boost have roughly constant ΔR. The dashed rectangles indicate the target sensitivity of this analysis.

The number of mu-jets and the number of muons in each mu-jet is used to classify different signal topologies (any ungrouped muons are ignored). A separate mass-peak fit is performed in the N-dimensional fundamental dimuon spectrum of each signal topology, where N is the number of fundamental dimuons per event. These topologies are:

(a) only one mu-jet per event:

- (a-1) two muons in the mu-jet with vector-sum $p_T > 80$ GeV/c, targeting models with a single high-momentum $m_1 \to \mu\mu$,
- (a-2) four muons in the mu-jet, targeting models with a low-mass m_2 decaying via $m_2 \to m_1 m_1 \to 4\mu$,
- (a-3) more than four muons in the mu-jet, for more complex models;

(b) two mu-jets per event:

- (b-1) each mu-jet contains exactly two muons, targeting a model with a heavy particle M decaying to two light particles m_1: $M \to m_1 m_1 \to 4\mu$ (this is the NMSSM signature),
- (b-2) one mu-jet contains two muons, the other contains four, targeting $M \to m_1 m_2$ with $m_1 \to \mu\mu$ and $m_2 \to m_1 m_1 \to 4\mu$,
- (b-3) both mu-jets contain four muons for $M \to m_2 m_2$,

(b-4) one mu-jet with more than four muons, for more complex models;

(c) more than two mu-jets per event, targeting even more complex models.

Mass-peak fits are used to search for a narrow resonance above background, with the background normalization determined as a free parameter in the fit. The signal is modeled as a narrow Crystal Ball resonance determined by detector resolution and muon final state radiation, and the background shape is derived from a mass template in background control samples. In cases with two or more fundamental dimuons per event, the signal is constrained to the diagonal in which the mass of all fundamental dimuons is nearly equal, while the background is more uniformly distributed through the space. If an m_1 mass peak is discovered in one of the topologies with two or more dimuons, then more complex fits will be performed to see if they belong to a cascade. A special 3-D fit to m_{h_1}, m_{a_1}, and m_{a_1} is performed for the NMSSM case $h_1 \to a_1 a_1 \to 2\mu, 2\mu$.

To avoid introducing complicated model-dependent efficiencies, signal regions are defined by kinematic cuts that avoid trigger turn-on curves and regions where the detector loses efficiency for muons that are very close to one another. Within the predefined acceptance regions, the efficiency depends only on muon pseudorapidity η. In brief, the acceptance cuts that we use are

- at least one muon with $p_T > 12$ GeV/c and $|\eta| < 0.9$ per event (muon barrel system trigger plateau);
- all other muons must have $p_T > 5$ GeV/c and $|\eta| < 2.4$ (offline reconstruction plateau).

The cuts on muon kinematics imply the following endpoints in mu-jet kinematics:

- at least one mu-jet with $p_T > 17$ GeV/c and $|\eta| \lesssim 0.9$ per event;
- all other mu-jets (if any) with $p_T > 10$ GeV/c and $|\eta| \lesssim 2.4$.

The η endpoints on mu-jets are only strict in the limit of highly boosted mu-jets, when the muons to which we applied the selection are nearly collinear. The mu-jet momentum minima are indicated with dashed lines in Fig. 1.

The trigger efficiency and offline muon reconstruction efficiency are derived as simple factors from $Z \to \mu\mu$ data using a tag-and-probe technique.

2 Trigger efficiency

For all signatures, we select events with the lowest unprescaled, unisolated, single-muon trigger available (see Appendix A for motivation). In the 2010A dataset (May–Aug 2010, 3 pb^{-1}), this is HLT_Mu9 and in the 2010B dataset (Sep–Oct 2010, 32 pb^{-1}), this is HLT_Mu11. (HLT_Mu11 trigger decisions do not exist in the 2010A dataset, so

the two datasets cannot be treated equally.) We require at least one $p_T > 12$ GeV/c, $|\eta| < 0.9$ muon offline to be insensitive to the shape of trigger turn-on curves and nearby-muon inefficiencies in the endcap.

The trigger response was studied in a generic way by simulating muon pairs with uniform mass, pair p_T, and pair η distributions (dimuon-gun MC). It is important to isolate dependencies of the efficiency on all physical variables in this unrealistic sample, as such a dependence would lead to model-dependent inefficiency in realisic cases.

In a dimuon-gun subsample with at least one $p_T > 12$ GeV/c muon (above the p_T turn-on curve for HLT_Mu9 and HLT_Mu11), the HLT_Mu11 efficiency versus dimuon mass, η, and p_T are shown in Fig. 2. The endcap region is inefficient for low-mass dimuons, and this inefficiency has a slight dependence on pair p_T.

To diagnose this further, we plot the efficiency as a function of how close the muon trajectories approach each other in the muon system (Fig. 3). The closeness of the muon trajectories is quantifed for $0.9 < |\eta| < 2.1$ on a plane at $|z| = 700$ cm (ME1/2), in terms of separation in azimuthal position $\Delta\phi = \phi_{\mu^+} - \phi_{\mu^-}$ and and radial position $\Delta r = r_{\mu^+} - r_{\mu^-}$: the efficiency drops by a factor of two when $|\Delta\phi| < 0.2$ and $|\Delta r/z| < 0.2$, though this efficiency loss is independent of leading muon p_T, as evidenced by the turn-on curve within the spot. Dimuons of different mass/momentum combinations sample this spot differently, as indicated by the labeled contour lines. Since the masses and momentum distributions of new physics dimuons is unknown, the endcap trigger efficiency cannot be quantified. That is why we require at least one above-threshold muon in the barrel per event. (This study was performed with a 2010B-like endcap trigger simulation— no ME1/1 singles and modified ghost suppression— though the conclusion is the same for the 2010A-like endcap trigger simulation.)

A Motivation for trigger choice

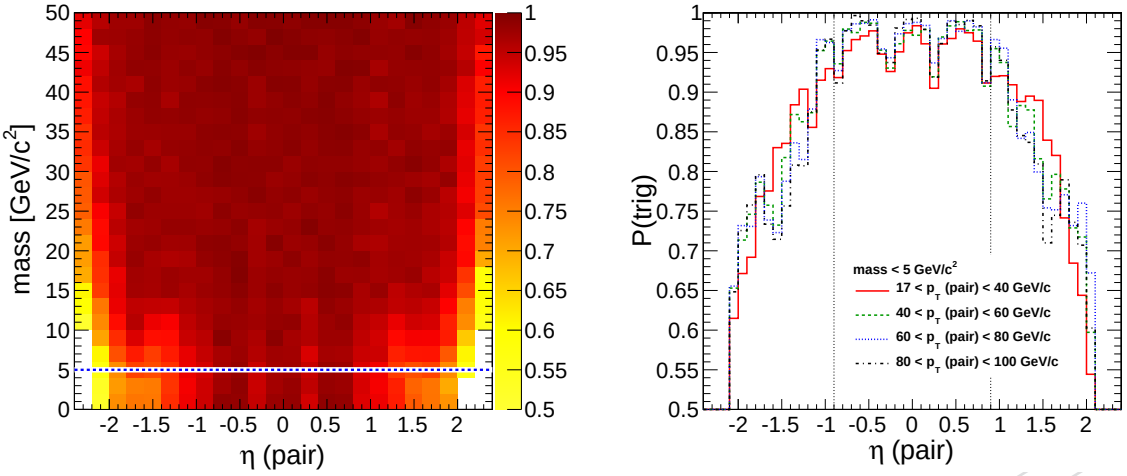

Figure 2: HLT_Mu11 trigger efficiency as a function of mass, momentum, and pseudorapidity of dimuons in a dimuon-gun simulation. In both plots, trigger efficiency is the fraction of event passing the trigger in a sample with at least one $p_T > 12$ GeV/c muon, the other unconstrained.

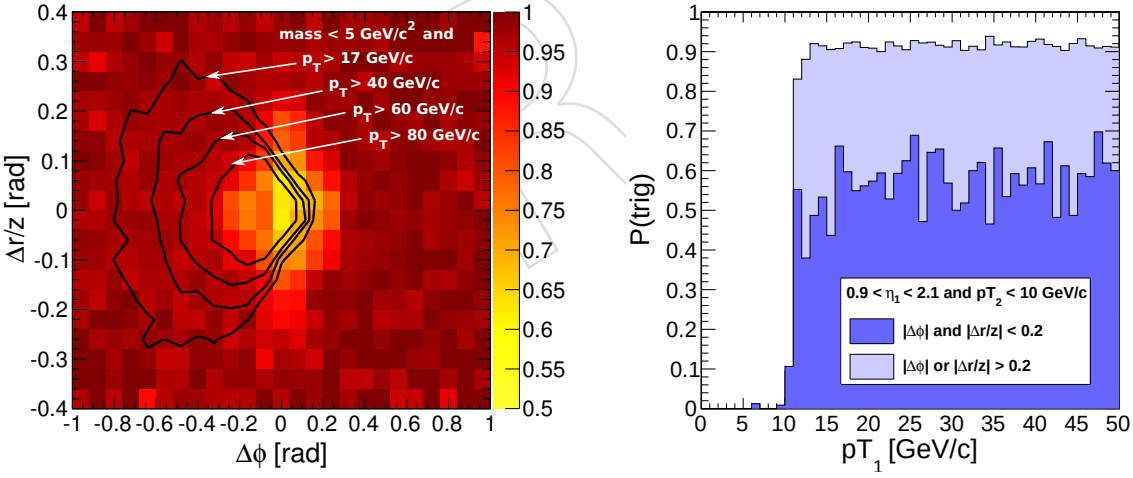

Figure 3: Diagnostic of HLT_Mu11 p_T dependence in $0.9 < |\eta| < 2.1$. Left: trigger efficiency (color scale) with one $p_T > 12$ GeV/c muon, the other unconstrained, as a function of separation of muons in the muon system. Different mass/momentum combinations (the labeled contour lines) sample this spot to differing degrees. The trigger turn-on curve in the spot is unaffected; it is the plateau efficiency that is lowered.